Wind tunnel study of the power output spectrum in a micro wind farm

Juliaan Bossuyt[1,2], Michael F. Howland[2], Charles Meneveau[2] and Johan Meyers[1]

[1]Department of Mechanical Engineering, KU Leuven, Celestijnenlaan 300, Leuven, Belgium.
[2]Department of Mechanical Engineering and Center for Environmental and applied Mechanics, Johns Hopkins University, 3400 North Charles Street, Baltimore, MD21218, USA.

E-mail: juliaan.bossuyt@kuleuven.com

Abstract. Instrumented small-scale porous disk models are used to study the spectrum of a surrogate for the power output in a micro wind farm with 100 models of wind turbines. The power spectra of individual porous disk models in the first row of the wind farm show the expected $-5/3$ power law at higher frequencies. Downstream models measure an increased variance due to wake effects. Conversely, the power spectrum of the sum of the power over the entire wind farm shows a peak at the turbine-to-turbine travel frequency between the model turbines, and a near $-5/3$ power law region at a much wider range of lower frequencies, confirming previous LES results. Comparison with the spectrum that would result when assuming that the signals are uncorrelated, highlights the strong effects of correlations and anti-correlations in the fluctuations at various frequencies.

1. Introduction

Unsteady flow properties and wind turbine wake interactions are a source of power output variability for wind turbines. Fluctuations in the power output are continuously present on scales from seconds to minutes due to turbulence, and on larger scales due to for example diurnal, synoptic and seasonal variations. The power output variability, characterized by the fluctuation amplitudes and accompanying ramp speeds, determines the necessary fill-in power required to follow a signal from the grid operator [2].

Summation over a large number of turbines reduces the power output fluctuations [10]. However, the power output of turbines in a wind farm can show a significant correlation, resulting in a non trivial reduction in the power output variability [14]. Field data [2] and a LES study [14] have shown that the spectrum of the aggregate power output follows a power law with a nearly -5/3 slope, similar to a Kolmogorov scaling for the inertial range of hydrodynamic turbulence.

In this study we make use of a large array of specially designed porous disk models for which the instantaneous thrust force of every model is measured as a surrogate for the power output. The micro-scale wind farm consists of 100 scaled models of wind turbines [5]. The power spectrum of the measured time signals is used to study the effect of spatial correlation in the individual signals on the total wind farm power output variability. This is made possible by the unique spatio- and temporal resolution of the measurement setup of a scaled large wind farm, within a controlled wind tunnel environment.

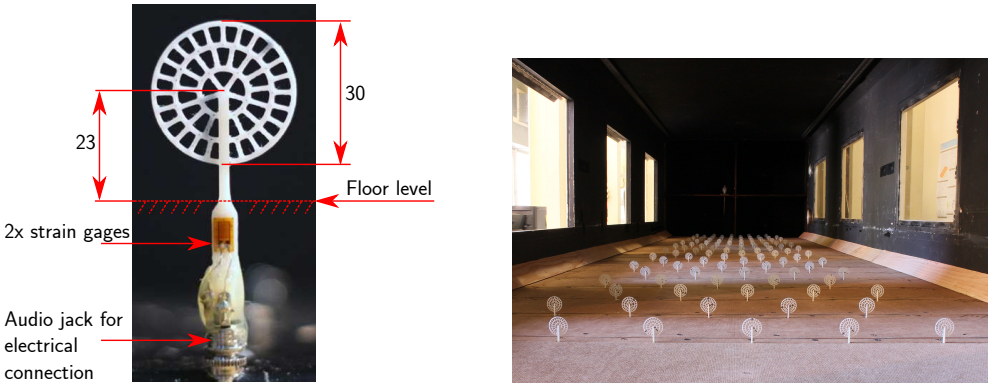

(a) (b)

Figure 1. (a) Porous disk model. (b) Photograph of the micro-wind farm in the Corrsin wind tunnel.

2. Experimental setup

Measuring the power output of a wind turbine or a wind farm with a high enough frequency response, to cover timescales as small as 16 seconds scaled to full scale, is made possible by making use of a specially designed porous disk model [5]. Porous disk models simulate the time averaged thrust force of an actual wind turbine on the flow. They have been used successfully in several studies to investigate the interaction between wind turbines and the boundary layer flow [3, 4, 5, 6, 9, 15] and more specifically have shown to represent adequately the mean kinetic energy transport of a rotor in the far wake where rotation is less important [7]. The bending moment of the model tower is measured with strain gages to deduce the thrust force as a surrogate for the turbine power output. The known thrust coefficient and a structural model are used to reconstruct the time signal of the incoming spatially averaged velocity. The equivalent power output signal is calculated from the reconstructed velocity signal for each measured porous disk model. Power signals are made independent of the assumed power coefficient by normalizing with the average power of the first row of spanwise aligned porous disk models (figure 2). The frequency response of the measurement goes up to the natural frequency of the model, approximately 200Hz.

The diameter of the porous disk is 0.03m and allows fitting a micro-wind farm with 100 of these instrumented models in the Corrsin wind tunnel [8]. The closed loop facility has a test section with a cross section of 0.9 x 1.2m and an approximate length of 10m. The side walls are adjusted outward to compensate for the boundary layer development. A smooth inflow with a background turbulence intensity of $TI_u \approx 0.12\%$ is provided by a primary contraction of 25 : 1 and a secondary contraction of 1.27 : 1. The turbulent boundary layer is then developed over a bottom surface of length 5m, after being tripped at the entrance. It reaches a height of $\delta_{99} = 0.18m$ where the micro wind farm starts. The measured roughness height is $z_0 = 0.9 \times 10^{-2}$mm, found by extrapolating the measured log-law velocity profile to the zero velocity at the wall. In this paper we only report results from a single wind speed (free stream velocity $U_\infty = 15.6$m/s). The measured friction velocity is $u_\tau = 0.6m/s$ at the beginning location of the wind farm, calculated from the slope of the log-law velocity profile and a Von Kármán constant of $\kappa = 0.4$. The corresponding geometric scaling for the porous disk model, compared to a full scale wind turbine with a diameter of 100m, is 1:3333. The porous disk model is designed to have a thrust coefficient of $C_T = 0.75 \pm 0.04$, similar to the typical thrust coefficient of a wind turbine working in the below-rated region (often referred to as region 2). In this operating regime the wind turbines are controlled to maximize their aerodynamic efficiency

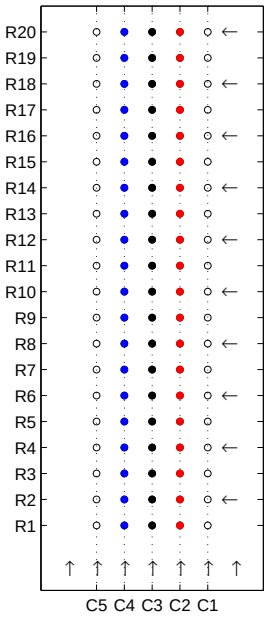

Figure 2. Row and column numbering for the wind farm model. The aligned layout is shown and the air flow is indicated by the vertical arrows. The staggered layout is constructed by shifting the even rows (as indicated by the horizontal arrows) half the spanwise spacing in the spanwise direction.

by adapting the rotor speed and pitch angle to the incoming wind velocity [1]. This is consistent with operating at a constant thrust coefficient.

The wind farm consists of 5 columns and 20 rows with a classical spacing of $S_x/D = 7$ in the streamwise direction and $S_y/D = 5$ in the spanwise direction. In this study we consider an aligned layout and a staggered layout, by shifting the even rows $2.5D$ in the spanwise direction. Data was acquired for the sixty models in the three central columns to focus the instrumentation resources on those models least affected by border effects (figure 2). Strain gage measurements were performed with an Omega iNET-430 16bit A/D converter and ten Omega iNET-423 voltage cards. The internal low pass filters of 4kHz are used to reduce high frequency noise. Due to the large number of simultaneous measurements, the acquisition rate was limited to 866Hz per model. This is lower than advised by the Nyquist frequency [11]. However, measurements for a single model with a sampling frequency satisfying the Nyquist theorem have shown that the aliasing error is small for the frequency range of interest. The duration of the power output measurement was approximately 30 minutes, to enable very well converged statistics, corresponding to 70 days in full scale. More information about the designed porous disk models and micro wind farm setup are discussed in a previous study [5].

3. Results and discussion

Two important characteristics of the power output variability which determine the necessary amount of fill-in power and the speed over which the fill-in power units have to react are the fluctuation amplitudes and the accompanying ramp speeds. These characteristics can be studied by calculating the power spectral density (PSD) of the power output signals to find the distribution of the variance in function of the frequency or corresponding time scale.

The PSD of a power output signal P_i of a porous disk model i is here calculated after

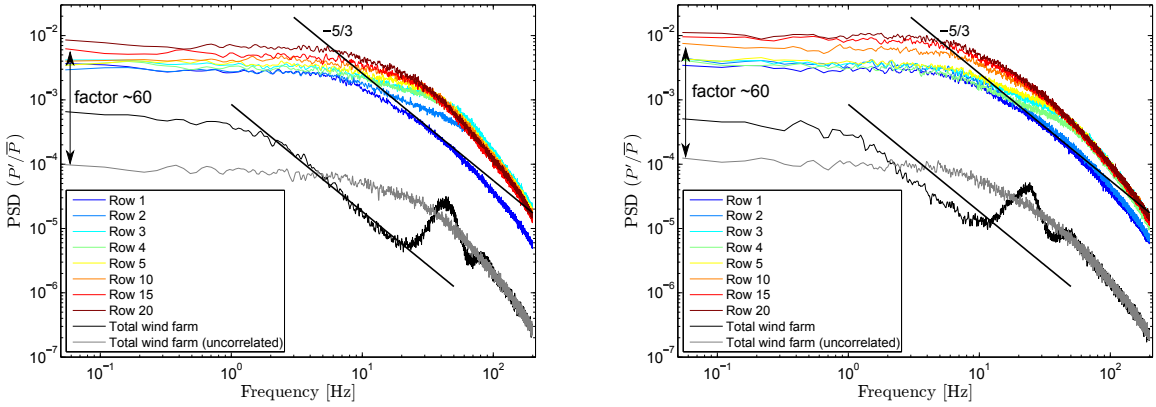

Figure 3. Power spectral density (PSD) measured for an aligned (a) and a staggered (b) wind farm layout. Colored lines are the average of the individual PSD's for all porous disk models in a specific row. The black line is the PSD of the total wind farm. The gray line is the PSD of the total wind farm, when the power signals are uncorrelated in time. Signals are uncorrelated by randomly shifting in time and assuming periodicity of the measurement interval.

normalizing the fluctuating part with the mean of the signal, according to:

$$PSD_i = PSD\left(\frac{P_i(t) - mean(P_i)}{mean(P_i)}\right). \tag{1}$$

The PSD is calculated with Matlab's pwelch function, averaging over 50 segments and windowed with the Hanning function. The calculated PSD are averaged over all porous disk models in a certain row.

The PSD of the total wind farm is calculated after summing up all individual power output time signals:

$$P_{WF}(t) = \sum_{i=1}^{60} P_i(t). \tag{2}$$

The PSD for the total wind farm power output is then calculated with the same normalization, the pwelch method and the same windowing parameters.

Figures 3 and 4 show the estimated PSD for two cases: an aligned and a staggered wind farm layout. The row-averaged PSD for single porous disk models are shown with the colored lines, according to the row number. The row-averaged PSD for a porous disk model in the first row is shown by the blue line. This can be considered as a measurement of the turbine output from the incoming flow characteristics with the application of a spatial filter by the porous disk. The spatial filter process of the porous disk is discussed and characterized in more detail in a previous study [5]. The spatial filtering explains why the slope for the highest frequencies in the measurement range (50-200Hz) is steeper than the expected $-5/3$ Kolmogorov slope. The PSD for downstream rows show a higher variance due to added turbulence from wakes of upstream models.

The black line, for the PSD of the total wind farm power output, shows a significant and non-trivial reduction in variability. The PSD shows an approximate power law behavior with a slope close to $-5/3$ in a frequency range of approximately $2 - 20$Hz. This confirms previous results from field experiments [2] and large eddy simulations [14]. Interestingly, this power law behavior

for the total wind farm power output extends to lower frequencies than observed for individual models. Considering that the velocity at hub height is approximately 10 m/s in the measurement, the lowest frequency of 2Hz corresponds to a length scale of 5m. This length scale is similar to the length of the entire wind farm model. As previously also observed in an LES study [14] a peak and a second harmonic peak are observed at frequencies corresponding to the convective flow time between two consecutive models. This peak is measured at a frequency of approximately 44Hz for the aligned and 23Hz for the staggered wind farm. Making use of the incoming velocity at hub height measured by the first row of porous disk models, and the streamwise spacing between streamwise consecutive models, the reduced frequency is approximately $S = fL/U = 0.86 - 0.9$ for both cases.

The non-trivial and frequency dependent reduction in variability indicates the importance of the power output cross-correlation between models in the wind farm. This was previously also reported by Sørensen et al. [13] and Stevens et al. [14]. To verify this effect the individual power signals were artificially uncorrelated in time by applying a random time shift. The PSD of the total power output by summing the uncorrelated time signals is shown by the gray line in figure 3.

From figure 3 we observe that the PSD of the total power output for uncorrelated signals (gray line) is approximately N=60 times smaller than the average of the individual porous disk PSD's (colored lines), independent of the frequency. This is in agreement with the following relation for the reduction of the variance $\sigma^2(\overline{x})$ of the mean of N normally distributed signals x_i in function of the correlation $corr_{ij}$ between the signals and the individual signal variances $\sigma^2(x_i)$ [10]:

$$\sigma^2(\overline{x}) = \frac{1}{N^2}\sum_{i}^{N}\sum_{j}^{N}\sigma(x_i)\sigma(x_j)corr_{ij}. \tag{3}$$

When there is no correlation between the signals ($corr_{ij} = 1$ for $i = j$ and $corr_{ij} = 0$ for $i \neq j$) the relation describes a reduction with N:

$$\sigma^2(\overline{x}) = \frac{1}{N}\sum_{i}^{N}\frac{\sigma^2(x_i)}{N}, \tag{4}$$

Where N is here the number of porous disk models: N= 60.

The higher variance for the PSD of the correlated wind farm power output (black line on figure 3) at frequencies lower than 5Hz, compared to the uncorrelated wind farm (gray line), indicates that the power output of porous disk models are correlated at these time scales. For higher frequencies ($5 - 20$Hz) we find that the porous disk models are anti-correlated, resulting in a lower variance. Finally, at the time scale corresponding to the convective flow time between two consecutive models, also shown by the peak, we notice a correlation between porous disk models.

Results for the staggered wind farm layout show similar trends, as seen in figure 3 (b). The peak has now shifted to a lower frequency due to the larger streamwise spacing. The power law region with a slope close to -5/3 now reaches to frequencies as low as 1 Hz. Considering a hub-height velocity of 10m/s, this corresponds to length scales of 10m, similar to the length of the wind tunnel test section.

For the current wind farm model, it was previously measured that the power output of streamwise aligned models are significantly correlated while the correlation in the spanwise direction is almost negligible [5]. This is in good agreement with measurements of the streamwise and spanwise correlation of a turbulent boundary layer [12]. The influence of this directional dependence of the cross-correlation between porous disk models on the power output variability is illustrated by figure 4. Colored lines represent the PSD of the total power output of each

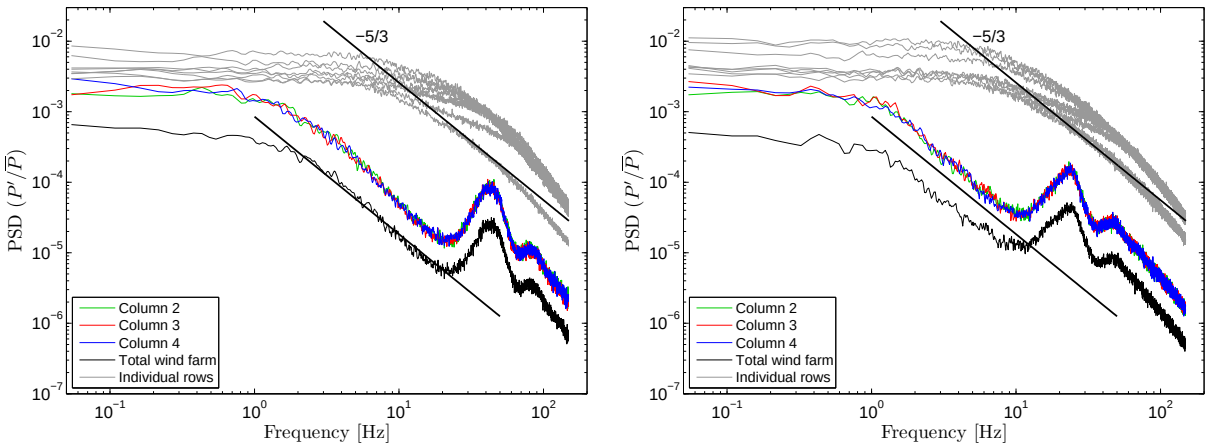

Figure 4. Power spectral density (PSD) measured for an aligned (a) and a staggered (b) wind farm layout. Colored lines are the PSD for the total power of each measured column in the wind farm. The black line is the PSD of the total wind farm. The gray lines are the average PSD for the individual rows, as shown in figure 3.

column (figure 2) of streamwise aligned porous disk models. The black line represents the PSD for the total wind farm and the gray lines represent the individual row-averaged porous disk PSD's, as shown in figure 3. Summation over all porous disk models in a column results in the non-trivial variability reduction described above. Summation over all columns, to find the total wind farm power output, reduces the variance with a constant factor of approximately 3. This confirms that the column-aggregate power outputs are uncorrelated due to a small spanwise correlation in the flow, while the significant streamwise correlation is a key factor in the non-trivial variability reduction.

4. Conclusions

The power output measured from small scale porous disk models in a wind tunnel experiment of a micro wind farm was analyzed by studying the power spectrum. An aligned and staggered layout were studied. A power law behavior for the power spectral density of the total wind farm power, with a nearly $-5/3$ slope, and a peak at the model-to-model flow timescale were observed. This confirms previous results from field data [2] and a LES study [14]. It is concluded that the designed experimental setup is capable of studying the power output variability and its dependence on the wind farm layout.

Depending on the layout, the $-5/3$ region for the total wind farm begins at a frequency of approximately 1-2 Hz, one order of magnitude smaller than measured by a single model in the first row. The reduction in variability is lower than for uncorrelated signals at low frequencies ($f < 2 - 5Hz$). This indicates a correlation between porous disk models at the corresponding time scales. For higher frequencies, but smaller than the model-to-model flow timescale, the reduction in variability is larger than for uncorrelated signals, indicating an anti-correlation. Finally, the peak at the model-to-model flow timescale, indicates a correlation.

It is concluded that the streamwise correlation plays a key factor in the non-trivial reduction of the power output variability.

Acknowledgments
Work supported by ERC (grant no. 306471, the ActiveWindFarms project) and by NSF (OISE-1243482, the WINDINSPIRE project).

References
[1] J. Aho, A. Buckspan, J. Laks, P. Fleming, Y. Jeong, F. Dunne, M. Churchfield, L. Pao, and K. Johnson. A tutorial of wind turbine control for supporting grid frequency through active power control. In *American Control Conference (ACC), 2012*, pages 3120–3131. IEEE, 2012.
[2] J. Apt. The spectrum of power from wind turbines. *Journal of Power Sources*, 169(2):369 – 374, 2007.
[3] S. Aubrun, G. Espana, S. Loyer, P. Hayden, and P. Hancock. Is the actuator disc concept sufficient to model the far-wake of a wind turbine? In *Progress in Turbulence and Wind Energy IV*, volume 141, pages 227–230. 2012.
[4] S. Aubrun, S. Loyer, P. Hancock, and P. Hayden. Wind turbine wake properties: Comparison between a non-rotating simplified wind turbine model and a rotating model. *Journal of Wind Engineering and Industrial Aerodynamics*, 120:1 – 8, 2013.
[5] J. Bossuyt, M. Howland, C. Meneveau, and J. Meyers. Measuring power output intermittency and unsteady loading in a micro wind farm model. In *34th Wind Energy Symposium*, page 1992, 2016.
[6] P. Builtjes. *Windturbine Wake Effects*. Division of Technology for Society, Netherlands Organization for Applied Scientific Research, 1979.
[7] E. H. Camp and R. B. Cal. Mean kinetic energy transport and event classification in a model wind turbine array versus an array of porous disks: Energy budget and octant analysis. *Physical Review Fluids*, 1(4):044404, 2016.
[8] G. Comte-Bellot and S. Corrsin. Simple eulerian time correlation of full-and narrow-band velocity signals in grid-generated,isotropicturbulence. *Journal of Fluid Mechanics*, 48(02):273–337, 1971.
[9] G. España, S. Aubrun, S. Loyer, and P. Devinant. Spatial study of the wake meandering using modelled wind turbines in a wind tunnel. *Wind Energy*, 14(7):923–937, 2011.
[10] G. Giebel. *On the benefits of distributed generation of wind energy in Europe*. VDI-Verlag, 2001.
[11] U. Grenander. *Probability and Statistics: The Harald Cramér Volume*. Alqvist & Wiksell, 1959.
[12] N. Hutchins and I. Marusic. Evidence of very long meandering features in the logarithmic region of turbulent boundary layers. *Journal of Fluid Mechanics*, 579:1–28, 2007.
[13] P. Sørensen, A. D. Hansen, and P. A. C. Rosas. Wind models for simulation of power fluctuations from wind farms. *Journal of wind engineering and industrial aerodynamics*, 90(12):1381–1402, 2002.
[14] R. J. A. M. Stevens and C. Meneveau. Temporal structure of aggregate power fluctuations in large-eddy simulations of extended wind-farms. *Journal of Renewable and Sustainable Energy*, 6(4), 2014.
[15] R. Theunissen, P. Housley, C. B. Allen, and C. Carey. Experimental verification of computational predictions in power generation variation with layout of offshore wind farms. *Wind Energy*, 18(10), 2015.